Remote Sensing of Environment 160 (2015) 222–234

Contents lists available at ScienceDirect

Remote Sensing of Environment

journal homepage: www.elsevier.com/locate/rse

Phytoplankton phenology indices in coral reef ecosystems: Application to ocean-color observations in the Red Sea

Marie-Fanny Racault [a,*], Dionysios E. Raitsos [a], Michael L. Berumen [b,c], Robert J.W. Brewin [a], Trevor Platt [a], Shubha Sathyendranath [a], Ibrahim Hoteit [d]

[a] Plymouth Marine Laboratory, Prospect Place, The Hoe, Plymouth PL1 3DH, United Kingdom
[b] Red Sea Research Center, King Abdullah University of Science and Technology, Thuwal 23955, Kingdom of Saudi Arabia
[c] Biology Department, Woods Hole Oceanographic Institution, 266 Woods Hole Rd, Woods Hole, MA 02543, USA
[d] Earth Science and Engineering (ErSE), King Abdullah University of Science and Technology, Thuwal 23955, Kingdom of Saudi Arabia

ARTICLE INFO

Article history:
Received 30 September 2014
Received in revised form 5 January 2015
Accepted 21 January 2015
Available online 18 February 2015

Keywords:
Phytoplankton phenology
Ocean-color remote sensing
ESA OC-CCI
Coral reef ecosystems
Monsoon
Ecological indicators
Red Sea

ABSTRACT

Phytoplankton, at the base of the marine food web, represent a fundamental food source in coral reef ecosystems. The timing (phenology) and magnitude of the phytoplankton biomass are major determinants of trophic interactions. The Red Sea is one of the warmest and most saline basins in the world, characterized by an arid tropical climate regulated by the monsoon. These extreme conditions are particularly challenging for marine life. Phytoplankton phenological indices provide objective and quantitative metrics to characterize phytoplankton seasonality. The indices i.e. timings of initiation, peak, termination and duration are estimated here using 15 years (1997–2012) of remote sensing ocean-color data from the European Space Agency (ESA) Climate Change Initiative project (OC-CCI) in the entire Red Sea basin. The OC-CCI product, comprising merged and bias-corrected observations from three independent ocean-color sensors (SeaWiFS, MODIS and MERIS), and processed using the POLYMER algorithm (MERIS period), shows a significant increase in chlorophyll data coverage, especially in the southern Red Sea during the months of summer NW monsoon. In open and reef-bound coastal waters, the performance of OC-CCI chlorophyll data is shown to be comparable with the performance of other standard chlorophyll products for the global oceans. These features have permitted us to investigate phytoplankton phenology in the entire Red Sea basin, and during both winter SE monsoon and summer NW monsoon periods. The phenological indices are estimated in the four open water provinces of the basin, and further examined at six coral reef complexes of particular socio-economic importance in the Red Sea, including Siyal Islands, Sharm El Sheikh, Al Wajh bank, Thuwal reefs, Al Lith reefs and Farasan Islands. Most of the open and deeper waters of the basin show an apparent higher chlorophyll concentration and longer duration of phytoplankton growth during the winter period (relative to the summer phytoplankton growth period). In contrast, most of the reef-bound coastal waters display equal or higher peak chlorophyll concentrations and equal or longer duration of phytoplankton growth during the summer period (relative to the winter phytoplankton growth period). The ecological and biological significance of the phytoplankton seasonal characteristics are discussed in context of ecosystem state assessment, and particularly to support further understanding of the structure and functioning of coral reef ecosystems in the Red Sea.

1. Introduction

Coral reefs are among the most biologically diverse ecosystems on Earth. They occupy less than 0.1% of the world's oceans, yet they host 25% of all the marine species (Spalding, Ravilious, & Green, 2001). Coral reefs deliver valuable and vital ecosystem services. They offer coastal protection, employment (through fisheries, recreation, and tourism), and are a major source of food for millions of people around the world (Hoegh-Guldberg, 1999). However, coral reefs are fragile ecosystems, facing serious threats from global climate change, marine acidification, destructive and unsustainable fishing practices, and water-polluting land-use activities (Hoegh-Guldberg et al., 2007; Wilkinson, 1999).

The Red Sea hosts thriving coral reef communities that have adapted to one of the most saline and warm basins in the world (Belkin, 2009; Cantin, Cohen, Karnauskas, Tarrant, McCorkle, 2010). The Red Sea is also unique because of its partial isolation from the Indian Ocean, its arid tropical climate, and its prevailing wind system regulated by the monsoon (Halim, 1969). During summer, northwesterly winds predominate in the Southern part of the Red Sea from June to September

* Corresponding author. Tel.: +44 175 263 34 34; fax: +44 175 263 31 01.
E-mail address: mfrt@pml.ac.uk (M.-F. Racault).

http://dx.doi.org/10.1016/j.rse.2015.01.019

(i.e. summer NW monsoon period), while during winter, in the southern Red Sea, prevailing winds reverse to southeasterly from October to May (i.e. winter SE monsoon period). Over the northern part of the Red Sea (North of 20°N), wind blow persistently from north-northwest throughout the year (Patzert, 1972). The Red Sea is further characterized by warm water temperature, which has been shown to be rapidly increasing since the mid-90s (from 27.4 °C on average during 1985–2003 to 28.1 °C on average during 1994–2007; Raitsos et al., 2011). These conditions make the Red Sea an excellent laboratory for studying the effects of the environment on marine organisms. In fact, the Red Sea has been shown not to be immune to the effects of global climate change and other disturbances, as evidenced by recent documentation of thermal coral bleaching events (e.g., Furby, Bouwmeester, & Berumen, 2013; Pineda et al., 2013) and historical crown-of-thorns starfish outbreaks (e.g., Riegl, Berumen, & Bruckner, 2013). Furthermore, in some regions, the majority of commercially targeted species have been overfished for decades (Jin, Kite-Powell, Hoagland, & Solow, 2012). High pressure is placed on apex predator populations, which are critical for ecological functioning in coral reefs, and are notably understudied in Red Sea ecosystems (Berumen et al., 2013; Spaet, Thorrold, & Berumen, 2012). For instance, the roving coral-grouper (*Plectropomus pessuliferus*) is highly targeted in the Red Sea, and a marked decline (or even disappearance in certain areas) has been shown, leading to the inclusion of this species into the International Union for Conservation of Nature (IUCN) Red List (Ferreira, Gaspar, Samoilys, Choat, & Myers, 2008).

Located at the base of the marine food web, phytoplankton support the functioning of coral reef ecosystems (Genin, Monismith, Reidenbach, Yahel, & Koseff, 2009; Wild, Jantzen, Struck, Hoegh-Guldberg, & Huettel, 2008; Wyatt, Lowe, Humphries, & Waite, 2010; Yahel, Post, Fabricius, & Genin, 1998), providing a source of food for many coral reef-associated organisms, including zooplankton, benthic grazers such as sponges (e.g., Richter, Wunsch, Rasheed, Kötter, & Badran, 2001; Yahel, Sharp, Marie, Häse, & Genin, 2003), bivalves (e.g., Yahel, Marie, Beninger, Eckstein, & Genin, 2009), and pelagic larvae (e.g., Erez, 1990; Johannes, 1978; Lo-Yat et al., 2011). In fact, the larvae of many marine species (including fish, crustaceans, mollusks and echinoderms) graze on phytoplankton during this vulnerable stage of their lives. Evidence that survival of gadoid fish larvae depends on the timing of the local spring bloom of phytoplankton has been demonstrated by Platt, Fuentes-Yaco, and Frank (2003) using a combination of satellite chlorophyll and in situ observations. Another characteristic example is the tight coupling reported between shrimp hatch time and the timing of remotely-sensed phytoplankton spring bloom peak in high-latitude ecosystems of the North Atlantic basin (Koeller et al., 2009). In a tropical ecosystem, Lo-Yat et al. (2011) have shown a significant positive relationship between remotely-sensed chlorophyll concentrations and the recruitment success of coral reef fish larvae. Assessing the phytoplankton phenology (timing of food availability) is important, as any changes may propagate up the marine food web, which may lead to trophic mismatch and alter the function of marine ecosystems (Edwards & Richardson, 2004).

To investigate trophic interactions in coral reef ecosystems, and to be able to detect anomalous trends or patterns, a comprehensive understanding of the seasonal variability (climatological cycle) of microscopic marine algae, phytoplankton, is required. In the Red Sea, general ecological research (Berumen et al., 2013) and long-term large-scale biological datasets are rare, with the latter mainly limited to satellite-based observations of ocean color (Acker, Leptoukh, Shen, Zhu, & Kempler, 2008; Brewin, Raitsos, Pradhan, & Hoteit, 2013; Labiosa, Arrigo, Genin, Monismith, van Dijken, 2003; Raitsos, Pradhan, Brewin, Stenchikov, & Hoteit, 2013). The color of the ocean is a good indicator of the primary photosynthetic pigment found in phytoplankton, chlorophyll (Sathyendranath & Platt, 1997). Over the past two decades, remote-sensing measurements of chlorophyll have provided unique information on surface marine phytoplankton, allowing us to monitor their distribution at high temporal and spatial resolution in coastal and open oceans (Blondeau-Patissier, Gower, Dekker, Phinn, & Brandoc, 2014). Chlorophyll concentration varies seasonally following the growth and decline of phytoplankton populations, which define the phytoplankton growing period. A suite of indices has been proposed to quantify phytoplankton seasonality (Platt & Sathyendranath, 2008) and to provide support to investigations on the composition, structure and functioning of the marine ecosystem (Racault, Platt, et al., 2014). The study of timing of periodical growth of phytoplankton populations relates to phenology. Phenological indices include timings of initiation, peak, termination, and duration of phytoplankton growing period (e.g., Racault, Le Quéré, Buitenhuis, Sathyendranath, & Platt, 2012). Several methods have been proposed to estimate these indices (see Ji, Edwards, Mackas, Runge, & Thomas, 2010 for a review). Conventionally, the methods involve a threshold criterion, which provides a boundary value to delineate initiation and termination of a phytoplankton growing period. The threshold criterion can be estimated directly from the remotely-sensed chlorophyll time-series (Henson, Robinson, Allen, & Waniek, 2006; Racault et al., 2012; Siegel, Doney, & Yoder, 2002; Thomalla, Fauchereau, Swart, & Monteiro, 2011), or after fitting a density function to the chlorophyll time-series (Platt, White, Zhai, Sathyendranath, & Roy, 2009; Vargas, Brown, & Sapiano, 2009; Zhai, Platt, Tang, Sathyendranath, & Hernández Walls, 2011; Sapiano, Brown, Schollaert Uz, & Vargas, 2012; González Taboada & Anadón, 2014; Ardyna et al., 2014), or performing a cumulative summation of the chlorophyll concentration (Brody, Lozier, & Dunne, 2013). Although different methods and threshold criteria may yield similar results, the choice of method and threshold requires scrutiny of the shape of the phytoplankton seasonal cycle. A further caution is that phenological studies require data well distributed in time (i.e. with few missing data), to enable resolution of timings of seasonal events with sufficient precision (Cole, Henson, Martin, & Yool, 2012; Land, Shutler, Platt, & Racault, 2014; Racault, Sathyendranath, & Platt, 2014).

Using SeaWiFS (Sea-Viewing Wide Field-of-View Sensor) and MODIS (Moderate Resolution Imaging Spectroradiometer) observations of chlorophyll, Acker et al. (2008) described the general seasonal variability of phytoplankton in the northern Red Sea. Using MODIS data, Raitsos et al. (2013) further examined phytoplankton seasonality in relation to environmental conditions in the Red Sea, and based on biological and physical characteristics, the latter authors proposed a partitioning into four provinces: the northern-Red Sea (NRS), the north-central Red Sea (NCRS), the south-central Red Sea (SCRS), and the southern Red Sea (SRS). However, in spite of the remarkable sampling coverage provided by remote-sensing technology, the presence of persistent clouds and atmospheric aerosol, sun-glint, and sensor saturation over sand have significantly limited data acquisition in the Arabian Sea and Red Sea regions. Specifically, during summer NW monsoon period, in addition to relatively frequent sand storms, the southern Red Sea is affected by hazy–cloudy conditions, which had prevented retrieval of useful remotely-sensed chlorophyll data until recently (Steinmetz, Deschamps, & Ramon, 2011). In 2014, the European Space Agency (ESA) Ocean-Colour Climate Change Initiative (OC-CCI) project produced and validated a consistent, stable, and error-characterized time-series of global ocean-color products based on merged SeaWiFS, MODIS and MERIS (MEdium Resolution Imaging Spectrometer) data (Hollmann et al., 2013; http://www.esa-oceancolour-cci.org). The progress made in the OC-CCI project has permitted improved coverage of remotely-sensed chlorophyll measurements in summer months in the Arabian Sea and southern Red Sea regions.

In the present study, we use ESA OC-CCI data to provide the first quantitative investigation of the phenology of phytoplankton in the Red Sea for both the winter and the summer growing periods. The research outcomes unfold as follows: 1) we assess and compare the spatial and temporal coverage of ocean-color observations from OC-CCI products with previously-available single-sensor SeaWiFS, MODIS and MERIS products; 2) we examine the performance of the ESA OC-CCI

chlorophyll retrieval algorithm in shallow reef-bound coastal waters of the Red Sea; 3) we develop an algorithm to compute a suite of phenology indices (i.e. timings of initiation, peak, termination and duration) in the entire Red Sea basin for the winter and summer phytoplankton growth periods; 4) we examine phytoplankton phenology in the vicinity of coral reefs, which we locate using sea-floor elevation data and the UNEP World Conservation Monitoring Centre (UNEP-WCMC) coral reefs dataset; 5) we analyze and compare phytoplankton phenological characteristics from open water areas located in the different ecological provinces and from coastal areas located in the vicinity of six large reef complexes; and 6) we review and discuss the significance of phytoplankton phenology for the functioning of coral reef ecosystems in the Red Sea.

2. Materials and methods

2.1. Datasets

2.1.1. Sea-floor elevation data

ETOPO5 sea-floor elevation data on a 5-minute latitude/longitude grid were obtained from the National Oceanographic and Atmospheric Administration (NOAA) at: http://www.ngdc.noaa.gov/mgg/global/etopo5.HTML. To be coherent with the spatial resolution of remote-sensing data, the sea-floor elevation data were then re-gridded to 4 km resolution using linear interpolation.

2.1.2. Coral reef distribution dataset

Global Distribution of Coral Reefs dataset (version 2010) compiled by the UNEP-WCMC was used to locate the position of coral reefs in the Red Sea. The dataset sources include the Millennium Coral Reef Mapping Project (IMaRS-USF (Institute for Marine Remote Sensing-University of South Florida) & IRD (Institut de Recherche pour le Developpement), 2005) and the World Atlas of Coral Reefs (Spalding et al., 2001). The dataset was obtained in ArcGIS vector format at http://data.unep-wcmc.org/datasets/13. It was then converted to NetCDF (Network Common Data Form) and gridded at 4 km resolution using the GRASS GIS software (http://grass.osgeo.org).

2.1.3. In situ chlorophyll data

Three independent datasets of in situ chlorophyll measurements were used to assess the performance of the ESA OC-CCI chlorophyll retrieval algorithm in reef-bound coastal and open waters of the Red Sea. The datasets, covering an extensive part of the study area, include: 1) In vivo fluorometric data on chlorophyll concentration collected from three research cruises during 2008, 2010 and 2011 (Brewin et al., 2013), as part of the Research Cruises expedition programme of the Red Sea Research Center (RSRC) of King Abdullah University of Science and Technology (KAUST); 2) In vivo Lidar fluorescence data on chlorophyll concentration in the Red Sea (Barbini et al., 2004) collected as part of the Mediterranean Sea, Indian and Pacific Oceans Transect (MIPOT) oceanographic campaign between Italy and New Zealand in November 2001; 3) In situ hyperspectral absorption and attenuation data collected on a flow-through system (Boss et al., 2013; Werdell, Proctor, Boss, Leeuw, & Ouhssain, 2013) during the Tara Oceans expedition in the Red Sea in January 2010. These in situ datasets were matched in time (day) and space (closest 4 km pixel) with the OC-CCI chlorophyll products and are presented in greater detail in Brewin et al., in review (Regional ocean-color chlorophyll algorithms for the Red Sea, paper in review in *Remote Sensing of Environment*, RSE-D-14-01018). Here, these datasets were used to evaluate the performance of OC-CCI chlorophyll products in shallow and deep-water regions, in the context of satellite estimates of phytoplankton phenology.

2.1.4. Sea-surface temperature remote sensing data

Level-3 mapped data of night-time (11 μm) sea-surface temperature (SST) from Aqua MODIS were used in this study. The 8-day climatology (period 2003–2008) at 4 km resolution product was obtained from the NASA ocean color website (http://oceancolor.gsfc.nasa.gov). MODIS SST datasets have been already used to monitor seasonal changes in marine temperatures in the Red Sea (Raitsos et al., 2013).

2.1.5. Ocean-color remote sensing data

Version 1 of ESA Ocean Colour CCI product comprising merged and bias-corrected MERIS, MODIS and SeaWiFS data was used in this study. OC-CCI reflectance data are processed using SeaDAS atmospheric-correction algorithm for SeaWiFS and MODIS (Fu, Baith, & McClain, 1998), and POLYMER algorithm for MERIS (Steinmetz et al., 2011). The level-3 mapped chlorophyll data were acquired at 4 km and 1-day resolution from http://www.esa-oceancolour-cci.org for the period Sep. 1997 to Dec. 2012. The data were then re-gridded to 8-day. This resolution provides a relatively high temporal resolution and limits missing data, which are important to improve accuracy and precision in the estimation of phenological indices (Racault et al., 2012; Racault et al., 2014).

Level-3 mapped data of chlorophyll were downloaded at 8-day resolution for the period 2003–2010 for each individual sensor SeaWiFS, MODIS and MERIS from the NASA ocean color archive (http://oceancolor.gsfc.nasa.gov/). MODIS (SeaDAS processing version 2013.1) and MERIS (SeaDAS processing version 2012.1) chlorophyll data were downloaded at 4 km resolution, while SeaWiFS (SeaDAS processing version 2010.0) data were downloaded at 9 km resolution (i.e. the highest available resolution for the mapped product in the archive).

Chlorophyll climatologies were computed and used as follows: 1) a ~15-year climatology Sep 1997 to Dec 2012 of OC-CCI chlorophyll at 4 km and 8-day resolution was constructed and used to estimate phenological indices (this is the longest continous ocean-color record available); 2) 8-year climatologies from Jan 2003 to Dec 2010 of OC-CCI, SeaWiFS, MODIS, and MERIS chlorophyll at 9 km and 8-day resolution were calculated and used in the comparison of data availability (this period corresponds to the time when all three satellite sensors SeaWiFS, MODIS and MERIS were coincidently recording data; see Fig. 2 in Results and discussion section). Linear interpolation was applied to perform spatial re-gridding from 4 km to 9 km. The periods used to calculate the climatologies were chosen to maximize the data coverage (i.e. 1997–2012, see assessment in Section 2.2) and to ensure overlap between recordings of individual sensors (i.e. 2003–2010).

2.2. Estimation of phenological indices

The threshold criterion method proposed and implemented herein has been developed to encompass the large variability of shapes in the phytoplankton growth encountered in the Red Sea. Preliminary investigation of the characteristics of the phytoplankton seasonal cycle in the Red Sea was performed using published literature based on in situ (Genin, Lazar, & Brenner, 1995; Levanon-Spanier, Padan, & Reiss, 1979) and remote-sensing observations (Acker et al., 2008; Labiosa et al., 2003; Raitsos et al., 2013), and by direct examination of the OC-CCI chlorophyll dataset. A threshold criterion method, such as presented in Racault et al. (2012), was adopted to estimate phenological indices of timing of initiation, peak, termination and duration of phytoplankton growth during both winter and summer growing seasons (Fig. 1). First, the 8-day chlorophyll climatology (period 1997–2012) is calculated, providing complete coverage of the annual cycle at every pixel in the Red Sea (i.e. no missing data). Then, for the winter and summer seasons, the timings of initiation and termination are defined as the times when chlorophyll concentration rises above and falls below a threshold criterion of median plus 10%. The median is computed at every pixel from the annual cycle (based on the 8-day chlorophyll climatology). The same threshold criterion is used to estimate the

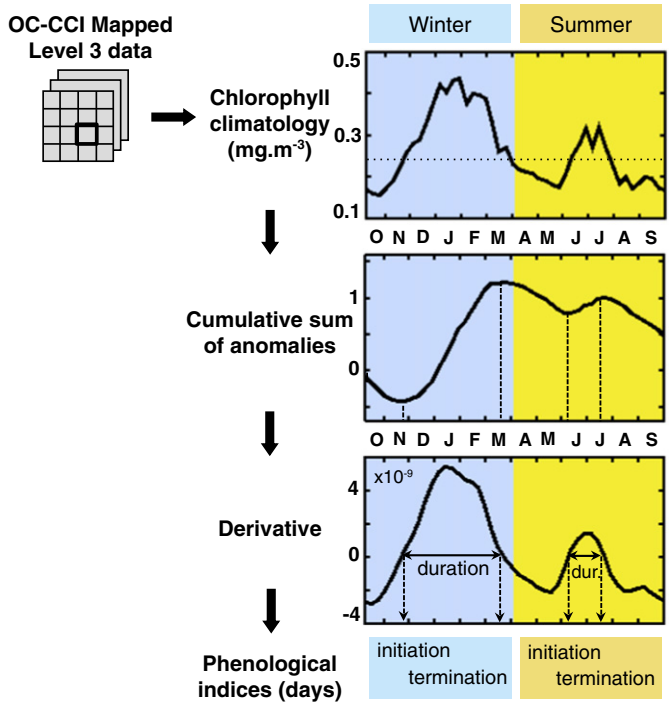

Fig. 1. Schematic representation of the method proposed to estimate phytoplankton phenological indices during winter (October to May) and during summer (June to September). The example time-series is from the pixel located at 41°E, 19°N. The chlorophyll climatology is computed based on the OC-CCI 8-day composites from Sep. 1997 to Dec. 2012. The median +10% threshold is calculated from the climatology. The anomalies are estimated as chlorophyll minus the threshold criterion and the cumulative sum of the anomalies is calculated. The derivative of the cumulative sum of anomalies is then computed. The times when the derivative is equal to zero are used to identify the timings of initiation and termination of the phytoplankton growing periods. Note that the timing of peak is searched between the timings of initiation and termination using the chlorophyll climatology. The same threshold criterion (median +10%, dashed line in the top panel) is applied to estimate both winter and summer growing periods. Further details on the method are provided in the main text (Section 2.2).

timings of initiation and termination during both the winter and summer seasons. The duration is calculated as the number of 8-day composites between the timings of initiation and termination. The timing of peak is detected as the time when maximum chlorophyll concentration is reached within the duration of a growing period.

Different threshold criteria were tested and limited sensitivity was observed in the estimations of timings of initiation and termination when thresholds ranged within median plus 5 to 15%. A lower threshold criterion may lead the algorithm to detect earlier (later) timings of initiation (termination) and in extreme cases, a nearly continuous growing period throughout the year may be estimated. On the other hand, a higher threshold criterion may exceed the maximum value in one of the growing periods relative to the other, with the result that the phenological algorithm may recover only one growing period.

The procedure to estimate the phenological indices is as follows (see Fig. 1 for a schematic representation). First, we subtracted the threshold criterion s from the 8-day climatology chlorophyll time-series Chl:

$$A = Chl - s. \quad (1)$$

The 8-day chlorophyll anomaly time-series is denoted A. When chlorophyll concentration is above the threshold, $A > 0$, and when chlorophyll concentration is below the threshold, $A < 0$. In the weeks preceding the commencement of the phytoplankton growing period, short pulses of chlorophyll associated with synoptic variability may be observed in the time-series. In these conditions, examination of cumulative chlorophyll anomalies C helps to avoid spurious estimation of timing of initiation:

$$C = \sum_i A_i, \quad (2)$$

A_i is the chlorophyll anomaly summed over 8-day periods i, starting at the beginning of the climatology. This method builds upon the benefits of using the cumulative sum approach (Brody et al., 2013; Greve, Prinage, Zidowitz, Nast, & Reiners, 2005), which has been shown to reduce potential "noise" or short pulses of chlorophyll data without filtering out any of the signal. Furthermore, the cumulative sum of anomalies method (Lozowski, Charlton, Nguyen, & Wilson, 1989) also allows us to identify persistent periods of chlorophyll increase above the threshold criterion s, which are used here to delineate a phytoplankton growing period. In the time-series of cumulative chlorophyll anomalies C, the growing periods appear as trends (i.e., an increasing trend when chlorophyll concentrations are above the threshold and a decreasing trend when chlorophyll concentrations are below the threshold; Fig. 1). Therefore, to estimate the timing when the trend changes direction, which corresponds to the time when chlorophyll rises above or falls below the threshold, we computed the derivative D of the cumulative anomalies of chlorophyll:

$$D = \frac{dC}{dt}. \quad (3)$$

The derivative time-series D was smoothed by applying a 3-week running average and the timings of initiation and termination were then readily estimated as the times when the derivative D was equal to zero. The phenology algorithm in the present study has been developed to estimate the main phytoplankton growing period in each season (i.e. winter and summer). If, during a season, a short pulse (<16 days) of chlorophyll reached concentrations above the threshold, then it would be detected by the algorithm but not output as a phenology metric.

The timings of initiation of phytoplankton growth were identified within two time intervals in the calendar year: 1) September to February for the winter growing period (phytoplankton growth had been demonstrated to peak between October and April, Raitsos et al., 2013); and 2) March to August for the summer growing period. The time boundaries selected to identify the timings of initiation were chosen in relation to the seasonal SST regime (González Taboada & Anadón, 2014), as a mean to connect variations in chlorophyll concentration to changes in environmental conditions. Indeed, temperature has been demonstrated as an important factor involved in the regulation of phytoplankton community structure (e.g., Bouman et al., 2003) and physiological processes (e.g., Saux Picart, Sathyendranath, Dowell, Moore, & Platt, 2014). Using the cumulative sum of anomalies climatological (modulo) time-series, the timings of termination were identified in the time intervals as follows: a) for a time-series characterized by two growing periods, the first timing of termination was identified in the time interval between the timing of initiation of the first growing period and the timing of initiation of the second growing period. Then, the second timing of termination was identified between the timing of initiation of the second growing period and the timing of initiation of the first growing period; b) for a chlorophyll time-series characterized by only one growing period, the timing of termination was identified as the next date when the derivative is equal to zero (after the timing of initiation). Finally, the timing of peak was searched in the time interval between the timings of initiation and termination using the chlorophyll climatology.

An evaluation of the cumulative sum of anomalies threshold method proposed here to estimate phytoplankton phenological indices, shows that two growing periods (winter and summer) were identified in 75% of the chlorophyll time-series available, whereas a single growing

period (either in winter or in summer) was identified in the remaining 25% of the chlorophyll time-series. In the present study, the main limit of the method to detect of one to two growing periods is dictated by the shape of the annual chlorophyll time-series (i.e. whether chlorophyll concentrations rise and fall above the threshold criterion during both the winter and summer growing seasons). The advantage to use the same threshold for both the winter and summer growing periods is that the inter-seasonal variability in the estimated phenological metrics can then be compared.

3. Results and discussion

3.1. Availability and performance of ocean-color remote-sensing observations in the Red Sea

Ocean-color observations from OC-CCI show a significant increase in spatial and temporal coverage compared with the results from single sensors SeaWiFS, MODIS and MERIS over the period 2003–2010 (Fig. 2). The climatological coverage of OC-CCI chlorophyll data is ≥75–80% throughout the year in the entire Red Sea basin, whereas from single sensors, in the Northern Red Sea, the coverage is around 65% (or less) throughout the year (with the exception of MODIS showing a coverage of nearly 75% during the winter months Nov–Jan). In the southern Red Sea, the climatological coverage from single sensors is around 50–55% (or less) in winter months, and this coverage drops to nearly 0% in the summer months (Jun–Sep). The extremely low data coverage in the southern Red Sea region reported from the single sensors is due to cloudy conditions and transport of dust particles in the atmosphere from the surrounding deserts during the northeast and southwest monsoon periods. In addition, the typical extreme heat during the summer months may induce hazy conditions. Hence, the region is particularly challenging for atmospheric-correction algorithms when processing MERIS, MODIS and SeaWiFS images, and pixels are flagged as of low quality in the SeaDAS atmospheric correction (Acker et al., 2008; Raitsos et al., 2013). The large increase in ocean-color data coverage especially in the southern regions and summer months observed in the OC-CCI dataset is due to the application of POLYMER algorithm to MERIS imagery (Steinmetz et al., 2011). The POLYMER algorithm is based on two models: 1) a polynomial atmospheric model representing the atmospheric scattering from large particles, aerosols, semi-transparent clouds and residual sun glint; and 2) a bio-optical ocean water reflectance model. These two models render the POLYMER algorithm robust to the effects of sun glint, semi-transparent clouds, and atmospheric dust aerosols, which occur during the monsoon, particularly in the Southern Red Sea region. This has led to a large increase in ocean-color data coverage in the OC-CCI chlorophyll data and permitted us for the first time to resolve the seasonal cycle of phytoplankton in summer months in the southern Red Sea. Finally, increased data coverage is highly beneficial, particularly to improve accuracy and precision in the estimation of phenological indices (Racault et al., 2014). The chlorophyll climatology estimated from the extended OC-CCI dataset (1997–2012) has permitted us to extract a complete annual cycle (i.e. no missing data in the climatology) at every pixel in the Red Sea.

Prior to analyzing phytoplankton seasonal cycle and estimating phenological indices, the performance of the OC-CCI chlorophyll retrieval algorithm was evaluated in shallow, reef-bound coastal waters of the Red Sea. The relationship between $\log_{10}$-tranformed chlorophyll from in situ and satellite measurements was statistically significant ($r = 0.82$ with $p < 0.05$ and $\Psi = 0.24$, where r is the Pearson correlation coefficient, p relates to the significance of this correlation ($p < 0.05$ mean statistically significant) and Ψ refers to the root-mean-sqaure-error) in coastal and/or shallow reef waters (i.e. waters with a depth <200 m; Brewin et al., 2010; Uitz, Claustre, Morel, & Hooker, 2006), and comparable to the results in

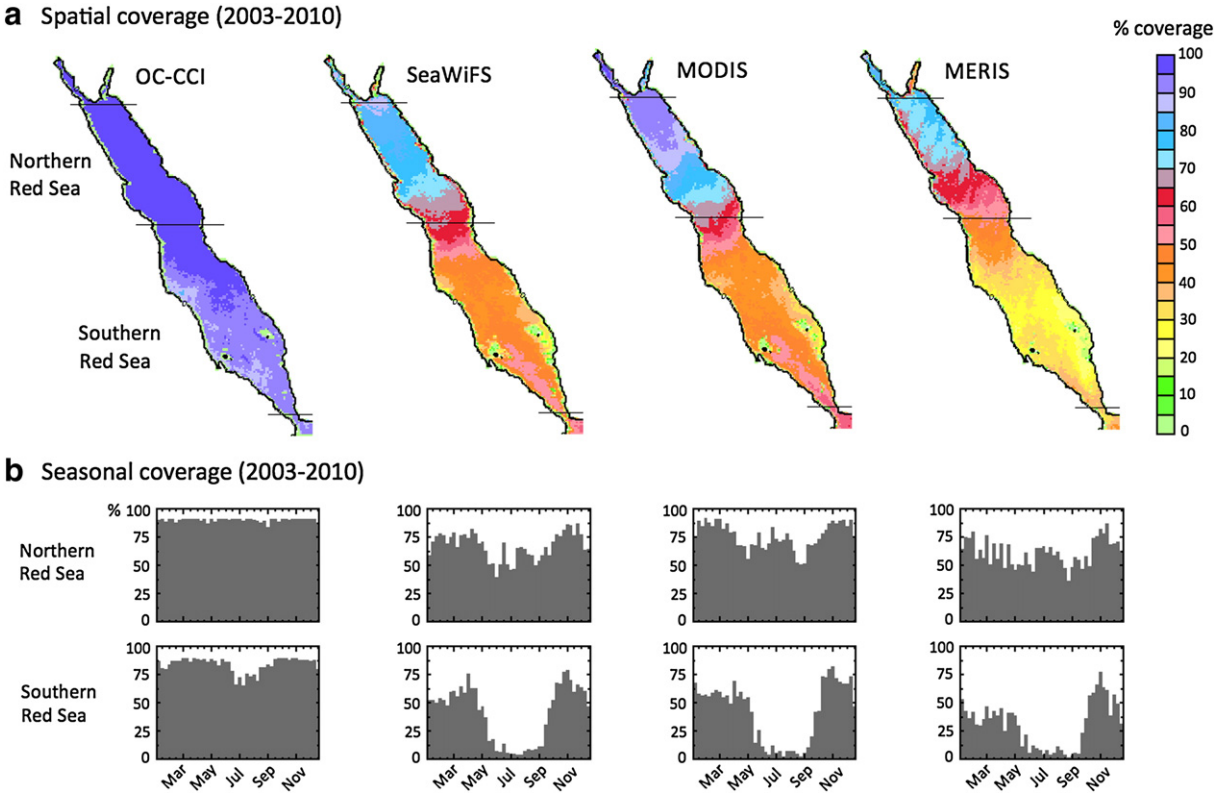

Fig. 2. Spatial and seasonal coverage of chlorophyll data for the period 2003–2010 for the merged product ESA OC-CCI (data processed using POLYMER atmospheric correction algorithm for MERIS, and using SeaDAS for SeaWiFS and MODIS), and the sensors SeaWiFS, MODIS and MERIS (data processed using SeaDAS atmospheric correction algorithm for all three sensors). a) Spatial coverage is computed as the relative percent number of 8-day chlorophyll composites available during 2003–2010; b) Seasonal coverage corresponds to the relative percent number of chlorophyll data available for each 8-day period during 2003–2010 over the Northern and Southern Red Sea regions.

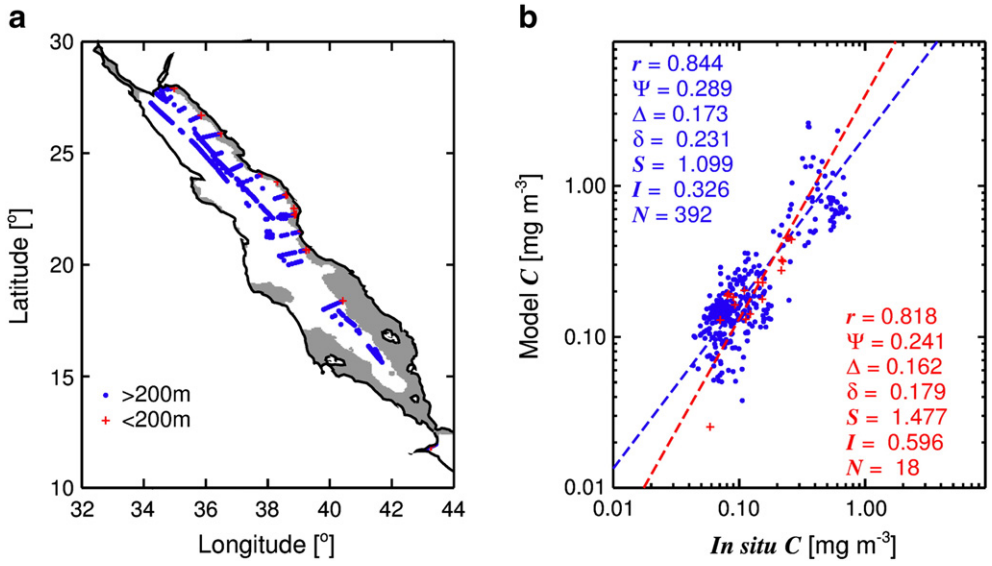

Fig. 3. a) Distribution of in situ and satellite match-up data used in the study. Red cross indicates match-up data located in water shallower than 200 m and blue dots indicate match-up data located in waters deeper than 200 m (the 200 m isobaths is used to delineate shallow reef-bound coastal waters, Brewin et al., 2010; Uitz et al., 2006); b) Scatter plots of the match-ups between in situ and satellite-derived chlorophyll (C) in the Red Sea using the OC-CCI algorithm for shallow waters (<200 m in red) and deeper waters (>200 m in blue). Univariate statistical tests were used and applied to $\log_{10}$-transformed chlorophyll data following Brewin et al. (2013). This included: the Pearson correlation coefficient (r); the root-mean-square-error (Ψ); the average bias between model and measurement (δ); the centre-pattern (or unbiased) root mean square error (Δ); the slope (S) and intercept (I) of a Type-2 regression; and the number of retrievals (N).

deeper open-ocean waters ($r = 0.84$ and $\Psi = 0.29$, Fig. 3). Previous comparison of match-ups of chlorophyll concentrations, measured in situ and from satellites, over extensive areas of the Red Sea indicated similar results to other standard chlorophyll products in the global ocean (Brewin et al., 2013). In optically complex waters, remotely-sensed chlorophyll data have known limitations, especially as yellow substances and non-algal particulate matter may not co-vary in a predictable manner with chlorophyll (Morel & Gentili, 2009). These factors may influence the retrieval of chlorophyll concentration, generally resulting in an overestimation (Blondeau-Patissier, 2009). However, not all high chlorophyll values in shallow waters are necessarily biased, as large coral reef complexes may be sources of either nutrients or chlorophyll-rich detritus that enhance phytoplankton production near the reefs (Genin et al., 2009; Labiosa et al., 2003; Levanon-Spanier et al., 1979; Sakka, Legendre, Gosselin, Niquil, & Delesalle, 2002; Wild et al., 2008; Wyatt et al., 2010; Yahel et al., 1998). The performance of the OC-CCI chlorophyll data in the Red Sea (both coastal and deep-waters, Fig. 3) is comparable with the performance of standard chlorophyll algorithms using large globally-representative datasets (see Brewin et al., In press, their Fig. 4), lending support to the use of the OC-CCI chlorophyll data to estimate phytoplankton phenology in the Red Sea.

3.2. Phytoplankton seasonality in the Red Sea

Based on the remotely-sensed observations from ESA OC-CCI, the northern provinces of the Red Sea (NRS and NCRS) exhibit

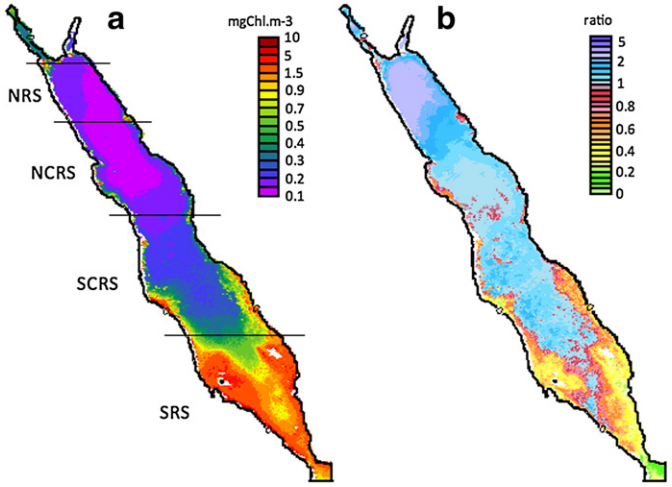

Fig. 4. Phytoplankton biomass in the Red Sea. a) Annual mean (climatology 1997–2012) chlorophyll concentration (in mg.m^{-3}) with the four provinces partitioning (Raitsos et al., 2013) overlaid: northern-Red Sea (NRS), north-central Red Sea (NCRS), south-central Red Sea (SCRS), and southern Red Sea (SRS); b) ratio of the mean chlorophyll concentration during winter SE monsoon (October to May) to the mean chlorophyll concentration during summer NW monsoon (June to September). When the ratio is greater than 1, the chlorophyll during the winter period is higher than the mean chlorophyll during the summer period.

lowest chlorophyll concentrations of 0.2 $mg.m^{-3}$ on average, which is characteristic of oligotrophic waters (Fig. 4a) and the southern provinces exhibit higher chlorophyll concentrations — an average of 0.4 $mg.m^{-3}$ in SCRS, and 1.7 $mg.m^{-3}$ in SRS. This increase in chlorophyll concentration from north to south is consistent with previous observations in the basin based on remotely-sensed chlorophyll concentration (Acker et al., 2008; Raitsos et al., 2013) as well as in situ chlorophyll and total pigment concentrations (McGill & Lawson, 1966 in Halim, 1969; Weikert, 1981). In the latter studies, phytoplankton pigment concentrations have been further reported to display a marked contrast between the two monsoon periods. Given the unique coverage provided by the OC-CCI dataset in the Red Sea region (Fig. 2), we investigated the ratio between mean chlorophyll concentrations during the winter SE monsoon period (October to May) and the summer NW monsoon period (June to September). Overall, it appears that in most of the open waters of the basin, average chlorophyll concentrations are higher during the winter compared with those during the summer (i.e. ratio greater than one; Fig. 4b). The highest ratio is found in the northern Red Sea province with values of nearly 2.5. An interesting result is that the ratio tends to be lower than one (or close to) in the waters adjacent to large reef complexes along the coast of the Red Sea (see Fig. 6 for position of coral reefs). This phenomenon is particularly apparent in the southern provinces of the Red Sea, where ratio values as low as 0.3 are observed, indicating that chlorophyll concentrations in reef-bound coastal waters are higher during the summer period compared with the winter period. Higher (or nearly equal) chlorophyll concentrations in reef-bound coastal waters during the warm period (Jun–Sep) have also been reported previously from in situ measurements in the Gulf of Aqaba (Levanon-Spanier et al., 1979, their Fig. 9; Yahel et al., 1998, their Table 2).

3.2.1. Phenological indices in open waters of the Red Sea

During winter, phytoplankton seem to flourish initially during the month of October in the southern part of the Red Sea (Fig. 5). The timing of initiation is slightly delayed in the northern part, with the winter phytoplankton growing period commencing in November. Chlorophyll concentrations peak between mid-December to mid-January throughout the entire Red Sea, except in the northwestern region of the NRS, which shows the latest peak timing at the end of March, and the southeastern region of the SRS, where the peak timing appears to occur earlier, around the beginning of October; coinciding with the intrusion of colder nutrient-rich waters from the Gulf of Aden (Churchill, Bower, McCorkle, & Abualnaja, In press; Mill & Post, 1981; Sofianos & Johns, 2003). The termination of the phytoplankton winter growing period occurs generally earlier in the southern part of the Red Sea (termination in March) compared with that in the northern part of the Red Sea (termination in April). These patterns of chlorophyll concentrations can be attributed to distinct physical regimes occurring in the Red Sea during winter: 1) in the northern part, nutrients are mainly supplied through convective vertical mixing (Labiosa et al., 2003; Mill & Post, 1981; Sofianos & Johns, 2003; Triantafyllou et al., 2014), which can sustain relatively long phytoplankton growing periods between 140 to 180 days; and 2) in the southern part, nutrient-rich waters are transported from the Gulf of Aden into the Red Sea, through horizontal advection driven by south-easterly winds (Churchill et al., In press; Mill & Post, 1981; Sofianos & Johns, 2003; Yao, Hoteit, Pratt, Bower, Zhai, et al., 2014), sustaining phytoplankton growth for a duration of approximately 120 to 160 days (Fig. 5, Table 1). In the central region of the Red Sea (around 20°N), an intermediate zone of wind convergence develops from October to April (Morcos, 1970), with the winds blowing from the north in the SSE direction, and from the south in the NNW direction (Patzert, 1972). These winds and the associated surface circulation trigger an initiation of the winter phytoplankton growing period (Raitsos et al., 2013), which is apparent in October (Fig. 5). The central region is further characterized by a north-south SST gradient (Yao, Hoteit, Pratt, Bower, Zhai, et al., 2014) and displays phytoplankton growing periods longer than 140 days in the central-west domain (Fig. 5, Table 1).

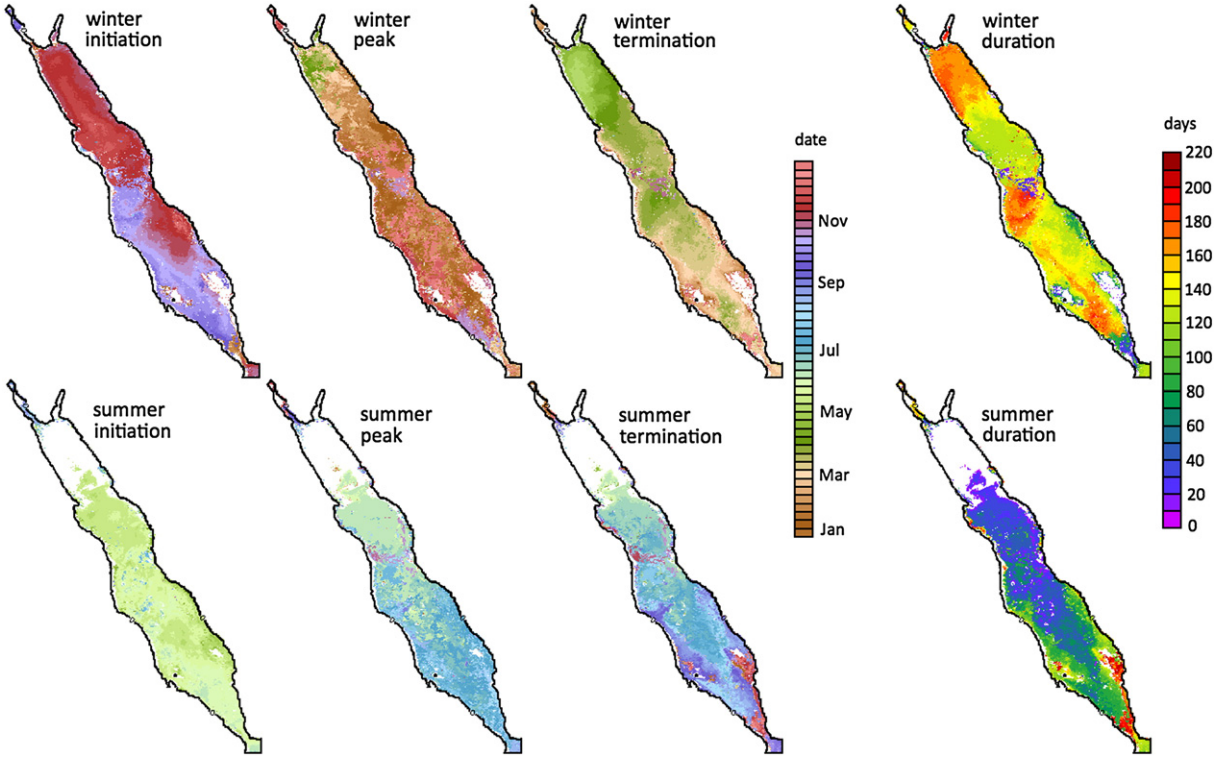

Fig. 5. Phenology of phytoplankton in the Red Sea. Winter (upper panels) and summer (lower panels) phytoplankton growing periods. White color indicates that no phytoplankton growing period was detected based on the threshold criterion method (see Materials and methods section for further information). The short duration (<20 days) reported in winter in the central part of the Red Sea are due to basin-wide anti-cyclonic eddies forming in the region (Johns, Jacobs, Kindle, Murray, & Mike, 1999), that generate short and particularly intense eddy-driven phytoplankton blooms, which may locally mislead the phenology detection algorithm implemented in this study (however, this feature is apparent for a small number of pixels and does not impede on the analysis of the phenology of phytoplankton in the entire basin).

Table 1
Mean phenology indices at six reef areas and in four biogeographical provinces in the Red Sea for winter and summer phytoplankton growing periods. Dates are within a standard error of ±8-day or less, except if indicated with a symbol $^{+}$ for ±16-day. The dates and maximum chlorophyll concentration are calculated as the mean of the observations in each area (see the area location in Fig. 6). No growing periods are reported during summer in Sharm El Sheikh reef (i.e. chlorophyll concentration remained below the bloom threshold criterion in more than 75% of the pixels in this area).

Site	Area (km^2)	Depth (m)	Indices winter					Indices summer				
			Initiation	Peak	Termination	Duration (days)	Max ($mg.m^{-3}$)	Initiation	Peak	Termination	Duration (days)	Max ($mg.m^{-3}$)
Siyal Islands	1472	130	01–08 Nov	11–18 Dec	25 Jan–01 Feb	96	0.37 ± 0.02	17–24 May	12–19 Jul	22–29 Sep	136	0.83 ± 0.06
Sharm El Sheikh	912	455	01–08 Nov	26 Feb–05 Mar	30 Mar–06 Apr	168	0.88 ± 0.20	–	–	–	–	–
Al Wajh Bank	1600	70	17–24 Nov	09–16 Jan	02–09 Feb	112 $^{+}$	1.07 ± 0.16	04–11 Jul	14–21 Sep	09–16 Nov $^{+}$	128	1.53 ± 0.14
Thuwal Reef	1664	50	16–23 Oct	01–08 Jan	26 Feb–05 Mar	120	0.50 ± 0.02	17–24 May	18–25 Jun	20–27 Jul	64	0.87 ± 0.10
Al Lith Reef	6528	100	09–16 Nov	09–16 Jan	18–25 Feb	88	0.81 ± 0.03	17–24 May	12–19 Jul	29 Aug–05 Sep	104	2.46 ± 0.10
Farasan Islands	7376	40	30 Sep–07 Oct	25 Nov–02 Dec	09–16 Jan	88	2.06 ± 0.06	17–24 May	20–27 Jul	22–29 Sep	144	7.12 ± 0.14
Northern Red Sea	2704	960	01–08 Nov	26 Feb–05 Mar	01–08 May	160	0.35 ± 0.00	–	–	–	–	–
Northern Central Red Sea	2704	1265	09–16 Nov	02–09 Feb	30 Mar–06 Apr	120	0.21 ± 0.00	25 May–01 Jun	10–17 Jun	26 Jun–03 Jul	32	0.23 ± 0.00
Southern Central Red Sea	2704	1430	16–23 Oct	09–16 Jan	14–21 Mar	144	0.4 ± 0.00	02–09 Jun	26 Jun–03 Jul	04–11 Jul	40	0.38 ± 0.01
Southern Red Sea	2704	955	30 Sep–07 Oct	17–24 Jan	06–13 Mar	144	1.03 ± 0.01	17–24 May	04–11 Jul	20–27 Jul	56	1.9 ± 0.05

During summer, phytoplankton exhibit a relatively homogeneous timing of initiation between the end of May and the beginning of June throughout the Red Sea, with the exception of the NRS province, where the summer growing period appears to be suppressed (Fig. 5). The chlorophyll concentration recorded in this province is lower in summer compared with the concentration recorded in winter and in the other provinces of the Red Sea (Fig. 4b). Furthermore, the NRS along with the central and deeper open ocean areas of the Red Sea are generally characterized by a relatively short (40 days or less) growing period (Fig. 5, Table 1). Chlorophyll concentrations show an apparent gradual progression in peak timing from mid-June in the NCRS to mid-July in the SCRS and SRS (Fig. 5). The observed increase in chlorophyll concentration occurs during the stratified nutrient-depleted summer period, and other sources of nutrient have been considered to explain this phenomenon (Raitsos et al., 2013). During this period, strong sea breezes and active anti-cyclonic eddies in the NCRS and SCRS provinces (Zhan, Subramanian, Yao, & Hoteit, 2014) may fuel nutrients and/or chlorophyll detritus from the coastal regions to the deeper central part of the Red Sea (Acker et al., 2008). Such processes may be further indicated in the low values of the winter to summer chlorophyll ratio (Fig. 4b), which are apparent with similar range of values (~0.8 to 1) in the reef-bound coastal waters and in local areas of the central Red Sea open and deeper waters.

3.2.2. Phenological indices in reef-bound coastal waters: case studies at six large reef complexes in the Red Sea

For each reef case study that follows, we provide: 1) a brief description of their socio-economic and/or conservation importance; 2) a precise evaluation of their phytoplankton phenological characteristics; and 3) a brief discussion on the significance of phenological indices to support the functioning of coral reef ecosystems. We use bathymetry data and the Global Distribution of Coral Reefs dataset (version 2010) to show the location of coral reef complexes in the coastal waters (i.e. waters with a depth <200 m; Brewin et al., 2010; Uitz et al., 2006). The chlorophyll seasonal cycle at each reef complex is shown in relation to the SST seasonal regime (see Fig. 6). Temperature is also used here as an indicator of surface water circulation patterns (e.g. resulting from upwelling, convective mixing) and to provide a frame of reference for the examination of the estimated phenological indices at the selected reef complexes.

3.2.2.1. Sharm El Sheikh. Sharm El Sheikh reef ecosystem provides major recreational and tourism services in Egypt, being visited by ten to hundred thousands of recreational divers each year (Hawkins & Roberts, 1994). It is located in the northern Red Sea province, around the latitudes 27.7–28.1°N, at the entrance to the Gulf of Aqaba.

The phenology of phytoplankton observed at Sharm El Sheikh reef is characterized by a prominent growing period occurring in winter (Fig. 6a). The timing of initiation of the winter growing period is estimated to occur between 1st and 8th of November and peak chlorophyll concentration (0.9 $mgChl.m^{-3}$) is observed between 26th February and 5th of March (Table 1), when SST is coolest and convective mixing is enhanced (Triantafyllou et al., 2014). Although this timing of initiation is relatively close to the winter timings of initiation observed in some of the other reefs examined in the present study (Table 1), the timing of termination at Sharm El Sheikh is markedly later, and hence the winter growing period shows the longest duration ~170 days (approximately five and a half months; Table 1). In the northern Red Sea (in the Gulf of Aqaba and in the vicinity of Sharm El Sheikh reefs), during the winter period, phytoplankton seasonality has been shown to be driven by deep convective mixing (Genin et al., 1995; Labiosa et al., 2003; Levanon-Spanier et al., 1979).

Upwelling-driven summer phytoplankton growth, reported in the Gulf of Aqaba (Labiosa et al., 2003) was detected in approximately 20% of the pixels (for which phenological information could be retrieved) in the Sharm El Sheikh reef area (Fig. 6, Table 1). This feature

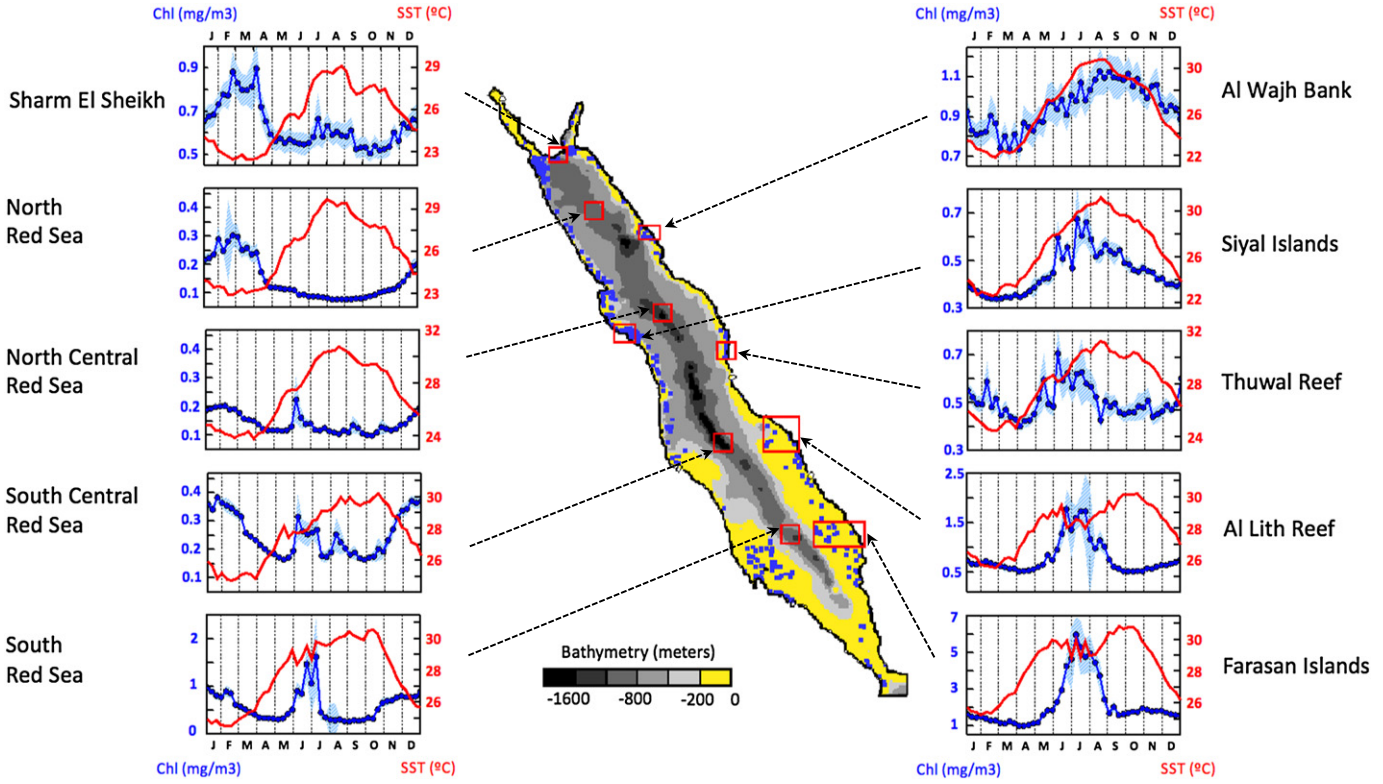

Fig. 6. Phytoplankton and sea-surface temperature seasonality in open and reef-bound coastal waters in the Red Sea. Central map: sea-floor elevation in the Red Sea with the distribution of coral reefs shown as blue squares (source: Global Distribution of Coral Reefs dataset, 2010). Side plots: Climatologies of sea-surface temperature (SST, in red) and chlorophyll concentration ±1 SE (in blue and shaded blue, respectively) at four open water sites and six reef complexes. The standard error (SE) represents the standard deviation of the error of the chlorophyll climatological mean calculated over the period 1997–2012.

suggests that the influence of coastal upwelling on phytoplankton dynamics may be limited to the Gulf of Aqaba and to the coastal waters adjacent of the entrance of the Gulf.

The large and prominent winter phytoplankton growing period compared with the limited or suppressed summer phytoplankton growth estimated in Sharm El Sheikh reef area is likely to have important implications for trophic interactions and pelagic-benthic coupling, which may turn to be quite different from what is occurring at other reef systems (see other case studies in the sections below, for which reef systems present equal or more prominent phytoplankton growth in summer compared with winter). Ecological studies have reported asynchronous spawning patterns for *Acropora* coral species in the Gulf of Aqaba (Shlesinger & Loya, 1985), while at other Red Sea reef complexes, these coral species appear to display synchronous spawning patterns (Hanafy, Aamer, Habib, & Baird, 2010; Bouwmeester, Khalil, De La Torre, & Berumen, 2011; Bouwmeester et al., 2014).

3.2.2.2. Siyal Islands. The Siyal islands reef area is located in the coastal waters of Sudan on the west side of the Red Sea around the latitudes 22.4–22.9°N in the north central Red Sea province. In the deeper central waters of this province, chlorophyll concentration appears higher in the winter period compared to the summer period (Fig. 4b). In contrast, the waters located in the vicinity of the Siyal Islands reef complex exhibit higher chlorophyll concentrations in summer (Fig. 4b; average ratio winter to summer chlorophyll for the Siyal Islands reef area is 0.77).

During the summer period, phytoplankton growth period appears to commence between 17th and 24th May on average in the reef area, and to reach peak chlorophyll concentration (0.8 mgChl.m^{-3}) between 12 and 19th July (Table 1). Timing of the chlorophyll peak precedes the SST maximum by approximately one and a half month (Fig. 6). This summer phytoplankton growing period may last ~140 days (nearly four months and a half), which is the longest duration of the six reefs examined in the present study.

During the winter period, phytoplankton growth is estimated to commence during 1st to 8th November, which is approximately one month after the estimated termination of the summer phytoplankton growth. Winter maximum chlorophyll concentration of 0.4 mg.m^{-3} is reached between 11th and 18th December (Table 1). At the Siyal Islands reef complex, winter phytoplankton growth is characterized by lower maximum chlorophyll concentration (nearly 2 times lower) and shorter duration (2 months shorter) compared with the summer growing period (Fig. 6).

Sudanese offshore coral reefs appear to harbor a significantly greater biomass than other reefs in the Red Sea (Spaet, 2014). These reefs seem to hold the only significant and persistent populations of large apex predators such as sharks and coral-groupers, although the reef structure and benthic communities appear to be similar to those of offshore reefs directly across the Red Sea (e.g., near Thuwal, see below) (M. L. Berumen, unpublished data). It remains unclear whether the longer duration of the summer phytoplankton growing period (i.e. longer period of food availability) has an influence on the trophic interactions at Siyal Islands reefs, but this warrants further investigation into the structure of the food web in these reefs relative to other Red Sea reefs.

3.2.2.3. Al Wajh Bank. The Al Wajh Bank reef complex is located on the east coast between the latitudes 25.4 and 25.8°N, at the boundary between the north Red Sea and the north central Red Sea provinces. It is a significant area for ecological conservation. The Al Wajh Bank consists of a large, shallow lagoon area nearly completely enclosed by reefs with very few openings to deeper water. Although tidal range in the Red Sea is generally very low, the volume of water contained inside this lagoon,

combined with the few channels opening to the adjacent deeper water, generates strong tidal currents in and out of the lagoon. At this reef complex, high chlorophyll concentrations had been previously reported (Acker et al., 2008). We further observe that chlorophyll concentrations are nearly equal or higher in summer compared with winter (Fig. 4b; average ratio winter to summer chlorophyll for the Wajh bank reef area is 0.98). The summer chlorophyll concentration follows the SST regime closely (Fig. 6).

During the warm period in summer, the timing of initiation of the phytoplankton growing period occurs between 4 and 11th July, which is noticeably later compared with the other reefs examined in the present study (which all display an apparent common timing of initiation between 17 and 24th May; Table 1). Maximum peak of 1.5 $mgChl.m^{-3}$ is reached later (compared with the other reefs), at the end of the summer months during the period 14th to 21st September, when SST is warmest (Fig. 6, Table 1). The summer phytoplankton growing period appears as one of the longest with a duration of ~130 days (approximately four months).

High chlorophyll concentration is also observed in the winter period, reaching maximum concentration of 0.9 $mgChl.m^{-3}$ between 9 and 16th January. Establishing a clear delineation between summer and winter phytoplankton growing periods at this reef complex was not straightforward using a threshold criterion method. In fact, the winter growing period is estimated to commence between 17 and 24th November, which is just one week after the estimated termination of the summer growing period in 9–16th November (Table 1). Winter chlorophyll concentration remains above the threshold criterion for 110 days (approximately three and a half months). Consequently, phytoplankton tends to be characterized by continuously elevated chlorophyll concentration (> median plus 10%) from mid-July until mid-February (Table 1, Fig. 6).

Many anecdotal reports suggest that the Al Wajh Bank is an important site for several types of megafauna, such as manta rays. Mantas are directly dependent on planktivorous food sources, and in the Red Sea appear to be reasonably site-restricted (Braun, 2013; Braun, Skomal, Thorrold, & Berumen, 2014). Hence, the hydrodynamic features and extended phytoplankton growing season observed at the Al Wajh Bank could have follow-on effects to larger zooplankton communities and subsequently to planktivorous filter feeders such as mantas. Further investigation will be required to elucidate this trophic linkage.

3.2.2.4. Thuwal Reefs. The complex of Thuwal reefs is situated between 21.9 and 22.4°N within the north central Red Sea province. In the waters adjacent to the reefs, a main winter and a secondary summer phytoplankton growing period are observed (Table 1, Fig. 6d). The amplitude of the phytoplankton blooms shows limited difference between winter (0.5 $mgChl.m^{-3}$) and summer (0.9 $mgChl.m^{-3}$), with winter to summer chlorophyll ratio of 1.1 on average in the area (Fig. 4b). However, the duration of the growing period is nearly double in winter, estimated to last ~120 days (approximately four months) compared to summer, estimated to last ~65 days (just over two months; Table 1).

During the winter period, phytoplankton growth period appears to commence during 16–24th October and chlorophyll concentration tends to peak between 1st and 8th January, when SST is cooler and nutrients are brought up to the surface by vertical mixing from the deeper water in the central part of the basin. During the summer period, phytoplankton growth shows an apparent start between 17 and 24th May, similar to most of the reefs examined in the present study, but the peak timing appears to occur noticeably earlier between 18 and 25th June (Table 1). Hence, in the area, summer chlorophyll peak precedes summer SST maximum by approximately two months (Fig. 6).

The Thuwal reefs complex is the location of a large and increasing number of research projects on coral reef ecosystems (Mervis, 2009). Understanding the local phytoplankton phenological cycle will provide useful information for a wide range of in situ experiments related to fishing practices (e.g., Jessen, Roder, Villa Lizcano, Voolstra, & Wild, 2013), observational studies of reef grazers (e.g., Khalil, Cochran, & Berumen, 2013) and further investigations on biogeochemical responses following coral mass spawning (e.g., Bouwmeester et al., 2014).

3.2.2.5. Al Lith Reefs. The Al Lith reef complex is located in the south central Red Sea province within the latitude band 19.2–20.2°N. It forms the northern end of the extensive Farasan Banks reef complex. Al Lith is emerging as a system of reefs with great importance on the eastern Red Sea coast, with value in both economic and research contexts. The site hosts manta rays (Braun et al., 2014) and the only known whale shark (*Rhincodon typus*) aggregation site in the Red Sea (Berumen, Braun, Cochran, Skomal, & Thorrold, 2014). Whale sharks, like manta rays, are large planktivorous fishes, and thus dependent on phytoplankton-zooplankton seasonal cycles.

During the summer period, the phytoplankton bloom begins around 17–24th May (as in most of the reefs examined in the present study; Table 1), and reaches maximum chlorophyll concentration of 2.5 $mg.m^{-3}$ in the period 12–19th July, when the increase in SST shows an apparent pause (Table 1, Fig. 6). This slow down in SST warming is likely to be caused by anti-cyclonic eddies, which form in the region and generally show strongest activity during summer (Fanning, Carder, & Betzer, 1982; Johns, Jacobs, Kindle, et al., 1999; Mill & Post, 1981; Yao, Hoteit, Pratt, Bower, Köhl, et al., 2014; Zhan et al., 2014). The eddies may provide a source of nutrients through resuspension and thus, sustain phytoplankton growth for a duration of ~100 days (just over three months; Table 1).

A winter phytoplankton growing period is also observed at Al Lith reefs, starting to develop during the period 9–16th November. Maximum winter chlorophyll concentration of 0.8 $mg.m^{-3}$ is reached during the period 9–16th January when SST is lowest (Fig. 6). The winter phytoplankton growing period lasts for ~90 days (approximately three months); possibly sustained by an inflow of cold nutrient-rich waters from the Gulf of Aden (Churchill et al., In press; Yao, Hoteit, Pratt, Bower, Zhai, et al., 2014).

Al Lith reefs appear to support two phytoplankton growing periods of equivalent duration (Table 1) but with very different amplitudes (Table 1; and Fig. 4b, ratio of winter to summer chlorophyll concentrations is 0.65 on average in the area). These phytoplankton phenological characteristics may play an important role in the aggregation of large planktivorous fish such as manta rays and whale sharks. In another reef ecosystem of the Great Barrier in Australia, the aggregation and abundance of whale sharks (*Rhincodon typus*) have been reported to occur during increased phytoplankton productivity and mass coral spawning (Taylor, 1996; Wilson, Taylor, & Pearce, 2001). The phenological indices presented at Al Lith reefs may help to elucidate trophodynamic links between phytoplankton availability and megafauna abundance.

3.2.2.6. Farasan Islands. The Farasan Islands complex is one of the most extensive island groups in the Red Sea, and is located in the latitude bands 16.4–17.1°N in the south Red Sea province. Many of the islands possess fringing coral reefs that show a notably different reef community composition compared with reefs from any of the other sites mentioned above. These reefs tend to have much more turbid water and a greater occurrence of macroalgae, both generally accepted as indications of greater local primary productivity. The summer peak chlorophyll concentration of 7.1 $mg.m^{-3}$ observed in the Farasan Islands is among the highest of the Red Sea (Fig. 6).

The phytoplankton phenological characteristics in the coastal waters of the Farasan Islands are very similar to these observed in the Al Lith reefs area. During the summer NW monsoon, the phytoplankton growing period starts in 17–24th May (same as Al Lith reef) and peak chlorophyll concentration is reached during 20–27th July (which is one week later than in Al Lith reef; Table 1). The duration of the summer growing period is longer (compared with the Al Lith reef group), lasting ~ 125 days (just over three months and a half; Table 1).

During the winter SE monsoon, chlorophyll concentration also shows a seasonal increase, albeit of markedly lower magnitude compared with the summer peak (i.e. ratio of winter to summer chlorophyll concentrations is 0.45 on average in the area, indicating that the summer chlorophyll concentration are more than double that of the winter (Fig. 4b)). The timing of initiation of the winter phytoplankton growing period is around 30th Sep to 7th October and maximum chlorophyll concentration of 2.1 $mg.m^{-3}$ is generally reached during the period 25th November to 2nd December. The winter timings of initiation and peak at the Farasan Islands are nearly one month earlier than the timings of growing period observed in Al Lith reefs. Furthermore, the duration of the winter growing period is also longer (compared with Al Lith reefs), lasting ~90 days (approximately three months). Although this area is shallow (and satellite chlorophyll algorithms may tend to overestimate in such regions, Fig. 2), this province is also the most strongly influenced by the inflow of cold waters from Gulf of Aden (Sofianos & Johns, 2003; Yao, Hoteit, Pratt, Bower, Zhai, et al., 2014).

In terms of population genetics, the Farasan Islands reef habitats appear to be substantially different from the other reef areas considered in this study. Although very few studies have considered the patterns of gene flow between the Farasan Islands and numerous other sites in the broader Red Sea, the greater productivity observed in the Farasan Islands and more broadly over the southern Red Sea province is likely to have profound implications for larval connectivity. Indeed, using chlorophyll concentration as a proxy for an environmental gradient, recent work on patterns of gene flow in anemonefish and sponges species indicate that the Farasan Islands are somewhat distinct genetically from sites in the Red Sea further north (Giles, 2014; Nanninga, Saenz-Agudelo, & Berumen, 2014). Further investigations on these population gene flow patterns may be carried out in relation with their biophysical habitats, which could be characterized statistically using phenological indices.

4. Conclusions and Perspectives

Phenological indices of timings of initiation, peak, termination and duration of the phytoplankton growing period estimated from ocean-color remote-sensing provide objective metrics to quantify phytoplankton seasonality in coral reef ecosystems. The phenological algorithm proposed in this study, based on a relative threshold method, is particularly relevant, as it allows us to encompass a broad diversity of shapes and concentration spectrum in chlorophyll seasonal cycles such as observed in open and reef-bound coastal waters in the Red Sea (Fig. 6). Specifically, the algorithm has been developed to resolve two phytoplankton growing periods per year. At each individual pixel, the winter and summer (if any) growing periods have been estimated relative to a unique threshold criterion, enabling inter-seasonal comparison of phenological indices. Furthermore, the index of duration of growing period (x-axis, with dimension [T]) carries information on phytoplankton availability that is conventionally contained in the measure of chlorophyll concentration (y-axis, with dimensions $[M\,L^{-3}]$). Thus, phenological indices bear the significant advantage to be robust to errors in absolute values of chlorophyll, which may arise from standard (i.e. based on globally-representative relationships) and sensor-specific chlorophyll retrieval algorithms, particularly sensitive in the optically complex waters of the Red Sea. However, notwithstanding the importance of precision and accuracy of the remote-sensing chlorophyll retrieval algorithm, the OC-CCI chlorophyll product was tested here for open and reef-bound coastal waters of the Red Sea and showed comparable performance with standard global-ocean chlorophyll retrieval algorithms (Fig. 2). In addition, the large gain in the number of chlorophyll observations during summer months demonstrated here with the usage of the POLYMER atmospheric correction algorithm (Fig. 3), has permitted us to provide the first comprehensive investigation of the phenology of phytoplankton in the Red Sea during the winter and summer periods.

Open waters of the northern Red Sea province are generally characterized by one main growing period during the winter, between December and April, which is driven by convective mixing. In contrast, open and deeper waters located in the central and south Red Sea provinces display two distinct growing periods: a primary growing period in winter, lasting approximately 4–5 months, and a secondary growing period of shorter duration in summer, lasting approximately 1–2 months. In these provinces, the winter growing period commences in December and finishes in March, and the summer growing period is estimated to begin in June and end in August. The winter growing period generally reaches higher amplitude, while the summer growing period is characterized by relatively low chlorophyll concentration (except in the southern shallow waters of the Red Sea, see below). The reef-bound coastal waters in the central and southern provinces of the Red Sea display different chlorophyll seasonality (compared to the open waters): highest chlorophyll concentrations are reached in summer (up to five times higher than in the winter) and the timing of termination of the summer growing period appears to occurs in September–October (which is one to two months later compared with the open waters of the central region, occurring in July, Fig. 5). The latter feature is also observed in the duration of the summer growing period, which is characterized by an apparent duration of 100 days or longer in the waters adjacent to the reefs compared with 50 days or shorter in the open and deeper water regions of the Red Sea. Thus, in reef-bound coastal waters, chlorophyll concentration appears to display larger peak in summer (relative to the winter peak), when SST is warmest and stratification is persistent (and nutrient supply from water circulation is likely to be minimum). This paradox suggests that nutrient sources from sediments (perhaps airborne deposition) and/or other organic compounds from coral reef complexes may be playing a considerable role in the enhancement of phytoplankton growth, and further investigations are required to shed light on this potential two-way mutual feedback mechanism between coral reefs and phytoplankton growth (Wild et al., 2008).

Monitoring and comprehensive analysis of phytoplankton seasonality, together with observations of reef fish spawning activity and larval survival, will allow us to improve our understanding of reef dwellers' recruitment strategies (Johannes, 1978) and to assess their sensitivities to environmental and climatic conditions (e.g., Wilson et al., 2001). Furthermore, the quantitative metrics provided by phytoplankton phenological indices should provide useful metrics to help us improve our understanding of coral reef biogeochemical pelagic-benthic coupling, aggregation of megafauna, and population gene flows (e.g., Nanninga et al., 2014). The phenological method proposed in this study may be extended to monitor inter-annual variability of phytoplankton seasonality in the Red Sea and in other reef ecosystems in the world oceans. It is anticipated that further studies - using advanced algorithms will enable serial assessment of the sensitivity of phytoplankton to environmental and climatic conditions (Raitsos et al., in press) and the possible impact on marine trophic interactions. This essential information will support the development of conservation plans and responsible stewardship of coral reef ecosystems (McCook et al., 2009; McKinnon, Williams, & Young, 2014).

Acknowledgments

This work is a contribution to the Ocean Colour Climate Change Initiative of the European Space Agency. The authors acknowledge Stéphane Saux Picart for discussion about phenology methods; James Dingle and Emma Carolan for technical support; the ESA Ocean Colour CCI Team for providing OC-CCI chlorophyll data; NASA for providing SeaWiFS, MODIS and MERIS chlorophyll data; NOAA for providing etopo5 sea-floor elevation data; and UNEP-WMCM, IMaRS-USF and IRD for providing coral reef distribution data. The research data presented in this paper are available

through the ESA LearnEO! online educational resources at: http://www.learn-eo.org/lessons/l11/.

References

Acker, J., Leptoukh, G., Shen, S., Zhu, T., & Kempler, S. (2008). Remotely-sensed chlorophyll a observations of the northern Red Sea indicate seasonal variability and influence of coastal reefs. *Journal of Marine Systems*, *69*, 191–204.

Ardyna, M., Babin, M., Gosselin, M., Devred, E., Rainville, L., & Tremblay, J. -E. (2014). Recent Arctic Ocean sea-ice loss triggers novel fall phytoplankton blooms. *Geophysical Research Letters*. http://dx.doi.org/10.1002/2014GL061047.

Barbini, R., Colao, F., De Dominicis, L., Fantoni, R., Fiorani, L., Palucci, A., et al. (2004). Analysis of simultaneous chlorophyll measurements by lidar fluorosensor, MODIS and SeaWiFS. *International Journal of Remote Sensing*, *25*, 2095–2110.

Belkin, I.M. (2009). Rapid warming of large marine ecosystems. *Progress in Oceanography*, *81*, 207–213.

Berumen, M. L., Braun, C. D., Cochran, J. E. M., Skomal, G. B., & Thorrold, S. R. (2014). Movement patterns of juvenile whale sharks tagged at an aggregation site in the Red Sea. *PloS One*. http://dx.doi.org/10.1371/journal.pone.0103536.

Berumen, M. L., Hoey, A. S., Bass, W. H., Bouwmeester, J., Catania, D., Cochran, J. E. M., et al. (2013). The status of coral reef ecology research in the Red Sea. *Coral Reefs*, *32*, 737–748.

Blondeau-Patissier, D., Brando, V. E., Oubelkheir, K., Dekker, A. G., Clementson, L. A., & Daniel, P. (2009). Bio-optical variability of the absorption and scattering properties of the Queensland inshore and reef waters, Australia. *Journal of Geophysical Research*, *114*, C05003. http://dx.doi.org/10.1029/2008JC005039.

Blondeau-Patissier, D., Gower, J. F. R., Dekker, A. G., Phinn, S. R., & Brandoc, V. E. (2014). A review of ocean color remote sensing methods and statistical techniques for the detection, mapping and analysis of phytoplankton blooms in coastal and open oceans. *Progress in Oceanography*. http://dx.doi.org/10.1016/j.pocean.2013.12.008.

Boss, E., Picheral, M. P., Leeuw, T., Chase, A., Karsenti, E., Gorsky, G., et al. (2013). The characteristics of particulate absorption, scattering and attenuation coefficients in the surface ocean: contribution of the Tara Oceans expedition. *Methods in Oceanography*, *7*, 52–62.

Bouman, H. A., Platt, T., Sathyendranath, S., Li, W. K. W., Stuart, V., Fuentes Yaco, C., et al. (2003). Temperature as indicator of optical properties and community structure of marine phytoplankton: Implications for remote sensing. *Marine Ecology Progress Series*, *258*, 19–30.

Bouwmeester, J., Baird, A.H., Chen, C. -J., Guest, J.R., Vicentuan, K.C., & Berumen, M.L. (2014). Multi-species spawning synchrony within scleractinian coral assemblages in the Red Sea. *Coral Reefs*. http://dx.doi.org/10.1007/s00338-014-1214-6.

Bouwmeester, J., Khalil, M.T., De La Torre, P., & Berumen, M.L. (2011). Synchronous spawning of *Acropora* in the Red Sea. *Coral Reefs*. http://dx.doi.org/10.1007/s00338-011-0796-5.

Braun, C.D. (2013). *Movement ecology of the reef manta ray Manta alfredi in the eastern Red Sea.* (MSc thesis) King Abdullah University of Science and Technology (58 pp.).

Braun, C.D., Skomal, G.B., Thorrold, S.R., & Berumen, M.L. (2014). Diving behaviors of the reef manta ray (*Manta alfredi*) in the Saudi Arabian Red Sea. *PloS One*, *9*, e88170.

Brewin, R. J. W., Raitsos, D. E., Dall'Olmo, G., Zarokanellos, N., Jackson, T., Racault, M. -F., et al. (2015). Regional ocean-colour chlorophyll algorithms for the Red Sea. (in review) *Remote Sensing of Environment* (RSE-D-14-01018).

Brewin, R.J.W., Raitsos, D.E., Pradhan, Y., & Hoteit, I. (2013). Comparison of chlorophyll in the Red Sea derived from MODIS-Aqua and in vivo fluorescence. *Remote Sensing of Environment*, *136*, 218–224.

Brewin, R. J. W., Sathyendranath, S., Hirata, T., Lavender, S. J., Barciela, R. M., & Hardman-Mountford, N. J. (2010). A three-component model of phytoplankton size class for the Atlantic Ocean. *Ecological Modelling*, *221*, 1472–1483.

Brewin, R. J. W., Sathyendranath, S., Müller, D., Brockmann, C., Deschamps, P. -Y., Devred, E., et al. (2015). The Ocean Colour Climate Change Initiative: III. A round-robin comparison on in-water bio-optical algorithms. *Remote Sensing of Environment*. http://dx.doi.org/10.1016/j.rse.2013.09.016 (in press).

Brody, S.R., Lozier, M.S., & Dunne, J.P. (2013). A comparison of methods to determine phytoplankton bloom initiation. *Journal of Geophysical Research*, *118*, 1–13.

Cantin, N. E., Cohen, A. L., Karnauskas, K. B., Tarrant, A. M., & McCorkle, D. C. (2010). Ocean warming slows coral growth in the central Red Sea. *Science*, *329*, 322–325.

Churchill, J.H., Bower, A.S., McCorkle, D.C., & Abualnaja, Y. (2015). The transport of nutrient-rich indian ocean water through the Red Sea and into coastal reef systems. *Journal of Marine Research* (in press).

Cole, H., Henson, S., Martin, A., & Yool, A. (2012). Mind the gap: The impact of missing data on the calculation of phytoplankton phenology metrics. *Journal of Geophysical Research*. http://dx.doi.org/10.1029/2012JC008249.

Edwards, M., & Richardson, A.J. (2004). Impact of climate change on marine pelagic phenology and trophic mismatch. *Nature*, *430*. http://dx.doi.org/10.1038/nature02808.

Erez, J. (1990). On the importance of food sources in coral reef ecosystems. In Z. Dubinsky (Ed.), *Coral reefs. Ecosystems of the world*. (pp. 411–417). Amsterdam, The Netherlands: Elsevier Science Publishers.

Fanning, K.A., Carder, K.L., & Betzer, P.R. (1982). Sediment resuspension by coastal waters: A potential mechanism for nutrient re-cycling on the oceans margins. *Deep-Sea Research*, *29*, 953–965.

Ferreira, B. P., Gaspar, A. L. B., Samoilys, M., Choat, J. H., & Myers, R. (2008). *Plectropomus pessuliferus*. *IUCN 2013. IUCN Red list of threatened species. Version 2013.2*.

Fu, G., Baith, K.S., & McClain, C.R. (1998). The SeaWiFS data analysis system. *Proceedings of the 4th Pacific Ocean Remote Sensing Conference (Qingdao, China, July 1998)* (pp. 73–79).

Furby, K.A., Bouwmeester, J., & Berumen, M.L. (2013). Susceptibility of central Red Sea corals during a major bleaching event. *Coral Reefs*, *32*, 505–513.

Genin, A., Lazar, B., & Brenner, S. (1995). Vertical mixing and coral death in the Red Sea following the eruption of Mount Pinatubo. *Nature*, *377*, 507–510.

Genin, A., Monismith, S.G., Reidenbach, M.A., Yahel, G., & Koseff, J.R. (2009). Intense benthic grazing of phytoplankton in a coral reef. *Limnology and Oceanography*, *54*, 938–951.

Giles, E. (2014). *Environmental effect on population genetic structure in the Red Sea as seen in the sponge, Stylissa carteri.* (MSc thesis) King Abdullah University of Science and Technology (47 pp.).

González Taboada, F., & Anadón, R. (2014). Seasonality of North Atlantic phytoplankton from space: Impact of environmental forcing on a changing phenology (1998–2012). *Global Change Biology*. http://dx.doi.org/10.1111/gcb.12352.

Greve, W., Prinage, S., Zidowitz, H., Nast, J., & Reiners, F. (2005). On the phenology of North Sea ichthyoplankton. *ICES Journal of Marine Science*, *62*, 1216–1223.

Halim, Y. (1969). Plankton of the Red Sea. In H. Barnes (Ed.), *Oceanography and marine biology, annual review, Vol. 7*. (pp. 231–275). George Allen & Unwin.

Hanafy, M.H., Aamer, M.A., Habib, A.B., & Baird, A.H. (2010). Synchronous reproduction of corals in the Red Sea. *Coral Reefs*, *29*, 119–124.

Hawkins, J.P., & Roberts, C.M. (1994). The growth of coastal tourism in the Red Sea: Present and future effects on coral reefs. *Ambio*, *23*, 503–508.

Henson, S.A., Robinson, I., Allen, J.T., & Waniek, J.J. (2006). Effect of meteorological conditions on interannual variability in timing and magnitude of the spring bloom in the Irminger Basin, North Atlantic. *Deep Sea Research, Part I*, *53*, 1601–1615.

Hoegh-Guldberg, O. (1999). Climate change, coral bleaching and the future of the world's coral reefs. *Marine and Freshwater Research*, *50*, 839–866.

Hoegh-Guldberg, O., Mumby, P. J., Hooten, A. J., Steneck, R. S., Greenfield, P., Gomez, E., et al. (2007). Coral reefs under rapid climate change and ocean acidification. *Science*. http://dx.doi.org/10.1126/science.1152509.

Hollmann, R., Merchant, C. J., Saunders, R., Downy, C., Buchwitz, M., Cazenave, A., et al. (2013). The ESA climate change initiative: Satellite data records for essential climate variables. *Bulletin of the American Meteorological Society*, *94*, 1541–1552.

IMaRS-USF (Institute for Marine Remote Sensing-University of South Florida), & IRD (Institut de Recherche pour le Developpement) (2005). *Millennium coral reef mapping project. Validated maps.* Cambridge (UK): UNEP World Conservation Monitoring Centre.

Jessen, C., Roder, C., Villa Lizcano, J. F., Voolstra, C. R., & Wild, C. (2013). In situ effects of simulated overfishing and eutrophication on benthic coral reef algae growth, succession, and composition in the central Red Sea. *PloS One*, *8*, e66992.

Ji, R., Edwards, M., Mackas, D.L., Runge, J.A., & Thomas, A.C. (2010). Marine plankton phenology and life history in a changing climate: Current research and future directions. *Journal of Plankton Research*, *32*. http://dx.doi.org/10.1093/plankt/fbq062.

Jin, D., Kite-Powell, K., Hoagland, P., & Solow, A. (2012). A bioeconomic analysis of traditional fisheries in the Red Sea. *Marine Resource Economics*, *27*, 137–148.

Johannes, R.E. (1978). Reproductive strategies of coastal marine fishes in the tropics. *Environmental Biology of Fishes*, *3*, 65–84.

Johns, W. E., Jacobs, G. A., Kindle, J. C., Murray, S. P., & Mike, C. (1999). *Arabian marginal seas and gulfs*. University of Miami RSMAS technical report 2000–01, 60.

Khalil, M.T., Cochran, J.E.M., & Berumen, M.L. (2013). The abundance of herbivorous fish on an inshore Red Sea reef following a mass coral bleaching event. *Environmental Biology of Fishes*, *96*, 1065–1072.

Koeller, P., Fuentes-Yaco, C., Platt, T., Sathyendranath, S., Richards, A., Ouellet, P., et al. (2009). Basin-scale coherence in phenology of shrimps and phytoplankton in the North Atlantic Ocean. *Science*, *324*. http://dx.doi.org/10.1126/science.1170987.

Labiosa, R. G., Arrigo, K. R., Genin, A., Monismith, S. G., & van Dijken, G. (2003). The interplay between upwelling and deep convective mixing in determining the seasonal phytoplankton dynamics in the Gulf of Aqaba: Evidence from SeaWiFS and MODIS. *Limnology and Oceanography*, *48*, 2355–2368.

Land, P., Shutler, J., Platt, T., & Racault, M. -F. (2014). A novel method to retrieve oceanic phenology from satellite data in the presence of data gaps. *Ecological Indicators*, *37*, 67–80.

Levanon-Spanier, I., Padan, E., & Reiss, Z. (1979). Primary production in a desert-enclosed sea — The Gulf of Elat (Aqaba), Red Sea. *Deep-Sea Research*, *26*, 673–685.

Lo-Yat, A., Simpson, S. D., Meekan, M., Lecchini, D., Martinez, E., & Galzin, R. (2011). Extreme climatic events reduce ocean productivity and larval supply in a tropical reef ecosystem. *Global Change Biology*, *17*, 1695–1702.

Lozowski, E.P., Charlton, R.B., Nguyen, C.D., & Wilson, J.D. (1989). The use of cumulative monthly mean temperature anomalies in the analysis of local interannual climate variability. *Journal of Climate*, *2*, 1059–1068.

McCook, L. J., Almany, G. R., Berumen, M. L., Day, J. C., Green, A. L., Jones, G. P., et al. (2009). Management under uncertainty: Guide-lines for incorporating connectivity into the protection of coral reefs. *Coral Reefs*, *28*, 353–366.

McGill, D.A. and Lawson, T.J. (1966). *The distribution of chlorophyll in the western Indian Ocean during the Northeast monsoon period*. Woods Hole Oceanographic Institution, Ref. 66-12, 69 pp. (unpublished manuscript).

McKinnon, A.D., Williams, A., & Young, J. (2014). Tropical marginal seas: Priority regions for managing marine biodiversity and ecosystem function. *Annual Review of Marine Science*, *6*, 415–437.

Mervis, J. (2009). The big gamble in the Saudi desert. *Science*, *326*, 354–357.

Mill, A.J.B., & Post, J. (1981). The physical environment. *Mining of metalliferous sediments from the Atlantis II Deep, Red Sea: Pre-mining environmental conditions and evaluation of the risk of the environment. Saudi-Sudanese Red Sea Joint Commission, 21-74, Report* (http://www.senckenberg.de/root/index.php?page_id=15250).

Morcos, S.A. (1970). Physical and chemical oceanography of the Red Sea. *Oceanography and marine biology, annual review, Vol. 8*. (pp. 73–202). H. Barnes, George Allen & Unwin.

Morel, A., & Gentili, B. (2009). The dissolved yellow substance and the shades of blue in the Mediterranean Sea. *Biogeosciences*, *6*, 2625–2636.
Nanninga, G.B., Saenz-Agudelo, P., & Berumen, M.L. (2014). Environmental gradients predict the genetic structure of a coral reef fish in the Red Sea. *Molecular Ecology*, *23*, 59–602.
Patzert, W.C. (1972). *Seasonal variations in structure and circulation in the Red Sea.* Hawai Institute of Geophysics (H16–73–3).
Pineda, J., Starczak, V., Tarrant, A., Blythe, J., Davis, K., Farrar, T., et al. (2013). Two spatial scales in a bleaching event: Corals from the mildest and the most extreme thermal environments escape mortality. *Limnology and Oceanography*, *58*, 1531–1545.
Platt, T., Fuentes-Yaco, C., & Frank, K. (2003). Spring algal bloom and larval fish survival. *Nature*, *423*, 398–399.
Platt, T., & Sathyendranath, S. (2008). Ecological indicators for the pelagic zone of the ocean from remote sensing. *Remote Sensing of Environment*, *112*, 3426–3436.
Platt, T., White, G.N., II, Zhai, L., Sathyendranath, S., & Roy, S. (2009). The phenology of phytoplankton blooms: Ecosystem indicators from remote sensing. *Ecological Modelling*, *220*. http://dx.doi.org/10.1016/j.ecolmodel.2008.11.022.
Racault, M. -F., Le Quéré, C., Buitenhuis, E., Sathyendranath, S., & Platt, T. (2012). Phytoplankton phenology in the global ocean. *Ecological Indicators*. http://dx.doi.org/10.1016/j.ecolind.2011.07.010.
Racault, M. -F., Platt, T., Sathyendranath, S., Ağirba , E., Martinez, Vicente V., & Brewin, R. (2014). Plankton indicators and ocean observing systems: Support to the marine ecosystem state assessment. *Journal of Plankton Research*. http://dx.doi.org/10.1093/plankt/fbu016.
Racault, M. -F., Sathyendranath, S., & Platt, T. (2014). Impact of missing data on the estimation of ecological indicators from satellite ocean-colour time-series. *Remote Sensing of Environment*. http://dx.doi.org/10.1016/j.rse.2014.05.016.
Raitsos, D. E., Hoteit, I., Prihartato, P. K., Chronis, T., Triantafyllou, G., & Abualnaja, Y. (2011). Abrupt warming of the Red Sea. *Geophysical Research Letters*, *38*, L14601.
Raitsos, D. E., Pradhan, Y., Brewin, R. J. W., Stenchikov, G., & Hoteit, I. (2013). Remote sensing the phytoplankton seasonal succession of the Red Sea. *PloS One*, *8*, e64909.
Raitsos, D. E., Yi, X., Platt, T., Racault, M. -F., Brewin, R. W. J., Pradhan, Y., et al. (2015). Monsoon oscillations regulate fertility of the Red Sea. *Geophysical Research Letters*. http://dx.doi.org/10.1002/2014GL062882 (in press).
Richter, C., Wunsch, M., Rasheed, M., Kötter, I., & Badran, M. I. (2001). Endoscopic exploration of Red Sea coral reefs reveals dense populations of cavity-dwelling sponges. *Nature*, *413*, 726–730.
Riegl, B., Berumen, M., & Bruckner, A. (2013). Coral population trajectories, increased disturbance and management intervention: A sensitivity analysis. *Ecology and Evolution*, *3*, 1050–1064.
Sakka, A., Legendre, L., Gosselin, M., Niquil, N., & Delesalle, B. (2002). Carbon budget of the planktonic food web in an atoll lagoon (Takapoto, French Polynesia). *Journal of Plankton Research*, *24*, 301–320.
Sapiano, M.R.P., Brown, C.W., Schollaert Uz, S., & Vargas, M. (2012). Establishing a global climatology of marine phytoplankton phenological characteristics. *Journal of Geophysical Research*, *117*, C08026. http://dx.doi.org/10.1029/2012JC007958.
Sathyendranath, S., & Platt, T. (1997). Analytic model of ocean color. *Applied Optics*, *36*, 2620–2629.
Saux Picart, S., Sathyendranath, S., Dowell, M., Moore, T., & Platt, T. (2014). Remote sensing of assimilation number for marine phytoplankton. *Remote Sensing of Environment*, *146*, 87–96.
Shlesinger, Y., & Loya, Y. (1985). Coral community reproductive patterns: Red sea versus the Great Barrier Reef. *Science*, *228*, 1333–1335.
Siegel, D.A., Doney, S.C., & Yoder, J.A. (2002). The North Atlantic spring phytoplankton bloom and Sverdrup's critical depth hypothesis. *Science*, *296*, 730–733.
Sofianos, S.S., & Johns, W.E. (2003). An Oceanic General Circulation Model (OGCM) investigation of the Red Sea circulation: 2. Three-dimensional circulation in the Red Sea. *Journal of Geophysical Research*, *108*, 3066.
Spaet, J.L.Y. (2014). *Integrating fisheries dependent and independent approaches to assess fisheries, abundance, diversity, distribution and genetic connectivity of Red Sea elasmobranch populations.* (PhD thesis) King Abdullah University of Science and Technology (163 pp.).
Spaet, J.L.Y., Thorrold, S.R., & Berumen, M.L. (2012). A review of elasmobranch research in the Red Sea. *Journal of Fish Biology*, *80*, 952–965.
Spalding, M.D., Ravilious, C., & Green, E.P. (2001). *World atlas of coral reefs*. Berkeley, USA: The University of California Press.
Steinmetz, F., Deschamps, P., & Ramon, D. (2011). Atmospheric correction in presence of sun glint: Application to MERIS. *Optics Express*, *19*, 571–587.
Taylor, J.G. (1996). Seasonal occurrence, distribution and movements of the whale shark, *Rhincodon typus*, at Ningaloo Reef, Western Australia. *Marine and Freshwater Research*, *47*, 637–642.
Thomalla, S.J., Fauchereau, N., Swart, S., & Monteiro, P.M.S. (2011). Regional scale characteristics of the seasonal cycle of chlorophyll in the Southern Ocean. *Biogeosciences Discussions*, *8*. http://dx.doi.org/10.5194/bgd-8-4763-2011.
Triantafyllou, G., Yao, F., Petihakis, G., Tsiaras, K. P., Raitsos, D. E., & Hoteit, I. (2014). Exploring the Red Sea seasonal ecosystem functioning using a three dimensional biophysical model. *Journal of Geophysical Research*. http://dx.doi.org/10.1002/2013JC009641.
Uitz, J., Claustre, H., Morel, A., & Hooker, S.B. (2006). Vertical distribution of phytoplankton communities in open ocean: An assessment based on surface chlorophyll. *Journal of Geophysical Research*, *111*, C08005.
Vargas, M., Brown, C.W., & Sapiano, M.R.P. (2009). Phenology of marine phytoplankton from satellite ocean color measurements. *Geophysical Research Letters*, *36*. http://dx.doi.org/10.1029/2008GL036006.
Weikert, H. (1981). The pelagic communities. *Mining of metalliferous sediments from the Atlantis II Deep, Red Sea: Pre-mining environmental conditions and evaluation of the risk of the environment. Saudi–Sudanese Red Sea Joint Commission, 100–155, Report* (http://www.senckenberg.de/root/index.php?page_id=15250).
Werdell, P.J., Proctor, C.W., Boss, E., Leeuw, T., & Ouhssain, M. (2013). Underway sampling of marine inherent optical properties on the Tara Oceans expedition as a novel resource for ocean color satellite data product validation. *Geophysical Research Letters*, *7*, 40–51.
Wild, C., Jantzen, C., Struck, U., Hoegh-Guldberg, O., & Huettel, M. (2008). Biogeochemical responses following coral mass spawning on the Great Barrier Reef: Pelagic–benthic coupling. *Coral Reefs*, *27*, 123–132.
Wilkinson, C.R. (1999). Global and local threats to coral reef functioning and existence: Review and predictions. *Marine and Freshwater Research*. http://dx.doi.org/10.1071/MF99121.
Wilson, S.G., Taylor, J.G., & Pearce, A.F. (2001). The seasonal aggregation of whale sharks at Ningaloo Reef, Western Australia: Currents, migrations and the El Niño/southern oscillation. *Environmental Biology of Fishes*, *61*, 1–11.
Wyatt, A.S.J., Lowe, R.J., Humphries, S., & Waite, A.M. (2010). Particulate nutrient fluxes over a fringing coral reef: Relevant scales of phytoplankton production and mechanisms of supply. *Marine Ecology Progress*. http://dx.doi.org/10.3354/meps08508.
Yahel, G., Marie, D., Beninger, P.G., Eckstein, E., & Genin, A. (2009). In situ evidence for pre-capture qualitative selection in the tropical bivalve *Lithophaga simplex*. *Aquatic Biology*, *6*, 235–246.
Yahel, G., Post, A.F., Fabricius, K., & Genin, A. (1998). Phytoplankton distribution and grazing near coral reefs. *Limnology and Oceanography*, *43*, 551–563.
Yahel, G., Sharp, J. H., Marie, D., Häse, C., & Genin, A. (2003). In situ feeding and element removal in the symbiont-bearing sponge *Theonella swinhoei*: Bulk DOC is the major source for carbon. *Limnology and Oceanography*, *48*, 141–149.
Yao, F., Hoteit, I., Pratt, L., Bower, A. S., Zhai, P., Köhl, A., et al. (2014). Seasonal overturning circulation in the Red Sea. Part-I: Model validation and summer circulation. *Journal of Geophysical Research*. http://dx.doi.org/10.1002/2013JC009331.
Yao, F., Hoteit, I., Pratt, L., Bower, A. S., Köhl, A., Gopalakrishnan, G., et al. (2014). Seasonal overturning circulation in the Red Sea. Part-II: Winter circulation. *Journal of Geophysical Research*. http://dx.doi.org/10.1002/2013JC009004.
Zhai, L., Platt, T., Tang, C., Sathyendranath, S., & Hernández Walls, R. (2011). Phytoplankton phenology on the Scotian Shelf. *ICES Journal of Marine Science*, *68*. http://dx.doi.org/10.1093/icesjms/fsq175.
Zhan, P., Subramanian, A., Yao, F., & Hoteit, I. (2014). Eddies in the Red Sea: A statistical and dynamical study. *Journal of Geophysical Research*, *119*, 3909–3925.